Online-Only Supplemental Materials

Section 1

e-Methods

Patient Measurements

Tonsillar displacement was measured according to the NINDS (National Institute of Neurological Disorders and Stroke) Common Data Elements for Chiari I Malformation (http://www.commondataelements.ninds.nih.gov). Tentorial angle measurements were taken using previously described methods.[9,19] Tentorial angle was defined as the angle between two intersecting lines: 1) one passing through the nasion and tuberculum sella and 2) the other along the straight sinus. Tentorium-Twining line angle was defined as previously described.[20] Measurements of tonsillar displacement, posterior fossa height, cervicomedullary kinking (Klaus index height), pontomedullary height, and platybasia were performed as previously described.[21] Basilar invagination was defined as the odontoid tip lying at least 5 mm above the McGregor line.[22] Volumetric posterior cranial fossa (PCF) measurements were made on T1-weighted sagittal MRI using OsiriX Imaging Software (Pixmeo; Geneva, Switzerland), using methodology that has been described extensively.[23-25] The osseous boundaries used to define the PCF included in the midline were the clivus from the dorsum sella to the basion, and the supra-occipital bone from the opisthion to the internal occipital protuberance (posterior tentorium); these were connected by lines across the foramen magnum (McRae's line), along the tentorium from the internal occipital protuberance to the posterior extent of the incisura, and from the dorsum sella to the posterior extent of the tentorial incisura. The internal osseous surface of the posterior fossa and the tentorium formed the outer boundaries of the region of interest on sections lateral to the midline. The volume of the PCF tissue contents was measured to include the volume of the cerebellar tonsils below the PCF. The volume of PCF tissue contents was measured to include tonsils below the PCF by extension of the ROI around them.

Bone Density Calculations (Hounsfield Units) from CT Abdomen/Pelvis

Bone density measurements were performed using OsiriX Imaging Software.[26-27] Regions of interest (ROI) included all trabecular regions of the for L5 vertebral body and S1, separately. Trabecular bone was separated from cortical bone using a freehand drawing tool that followed the endocortical boundary, excluding peripheral vestiges of the growth plate. Relative density was determined by the average Hounsfield Unit measured for the VOI.

Ex Vivo MRI of Head and Spine

The eviscerated cadavers were placed in a 20 mm *i.d.* NMR tube and submerged in Fluorinert (Service Chemicals, North Andover, MA). The head was centered in a 20 mm transmit-receive MRI probe and positioned in 14 T (Bruker Biospin Inc. Billerica, MA) vertical scanner. A navigator set of scan in three mutually perpendicular directions were acquired to envisage the brain area. A 3-dimensional volume (Field of View 25.6 ^{3} mm^3) encompassing the brain was selected using these pilot images and a 3D, T_1 weighted FLASH image (Echo time/repetition time = 5.5/50 ms, flip angle = 30^0, isotropic resolution = 37.5 mm) was acquired. The acquired images were displayed and analyzed using the scanner software.

Ex Vivo MicroCT of Head and Spine

Micro-CT of mouse anatomy was performed with a Bruker SkyScan1172 Micro-CT (Micro Photonics, Inc. Allentown PA, USA, SkyScan, Kontich, Belgium) with the X-ray source (focal spot size, 4 µm, energy range 20-100 kV) biased at 65kV/153 uA and with a 0.5 mm Al filter to reduce beam hardening. The images of the microfil perfused mice were acquired with a pixel size of 13.53 um, with the camera to source distance of 345.233 mm and an object to source distance of 259.500 mm. The scan orbit was 180 degrees with a rotation step of 0.4 degrees. Six frames were averaged for each projection with an exposure time of 1600 ms per frame.

Two non-perfused sets of mice, containing 2 WT and 2 Mutants received micro-CT imaging of the sacrum. The two sets were scanned using different resolutions; 5.95 um and 13.53 um. The former resolution was used to evaluated only the S1 vertebral body in ex vivo isolated spine samples. The latter was used to evaluate all vertebral bodies of the sacrum in whole intact ex vivo mice. The high resolution was scanned using 4 frame averaging with a exposure time of 590 ms. The lower resolution used 6 frame averaging with a exposure time of 1600 ms. Reference scans were used to calibrate to bone mineral density. The reference phantoms (Bruker-microCT, Kontich, Belgium)

contain 0.25 and 0.75 g.cm-3 CaHA evenly mixed in epoxy resin rods which were of similar diameter to the scanned bones to minimize beam hardening error.

Reconstruction was carried out with a modified Feldkamp2 algorithm using the SkyScan NRecon software. Ring artefact reduction and beam hardening correction were applied. Volume rendered 3D images were generated using an RGBA transfer function18 in SkyScan CT-Voxel ("CTVox") software.

Bone Mineral Density Calculation in Disease Mouse Model

ROI selection and segmentation to binary analysis was all performed using SkyScan CT-Analyser ("CTAn") software. ROI was determined using CTAn custom processing feature. Automatic (Otsu method) thresholding was applied to each sample in 3D space. The despeckle/sweep tool was applied to each image in 3D space to remove the all but the largest object in the scan, ie. the sacrum. An adaptive 2D ROI shrink-wrap function was applied to each scan. The resulting ROI combined with the original 2D images were analyzed for density using the appropriate calibration parameters.

Histology and Immunohistochemistry

Formalin fixed, paraffin-embedded tissue specimens from mice were cut in 5 μm sections that were placed on glass slides. After deparaffinization in xylene and subsequent rehydration in a series of graded ethanol baths, slides were boiled in citrate buffer for antigen retrieval. Tissue sections were blocked then incubated with HIF2α primary antibody (Abcam [ab109616], 1:500 ab:PBST) overnight at 4°C. Slides were then incubated with HRP-conjugated anti-rabbit IgG and developed using DAB substrate (Dako) using manufacturer's methods. Specimens were counter-stained using hematoxylin and dehydrated in ethanol. Additional H&E staining was performed on adjacent sections. Histological slides were viewed using a Nikon Eclipse Ci; images were digitally stored at 2x and 4x magnification using Nikon DS-L4 software.

Section 2

Supplemental Figures and Tables

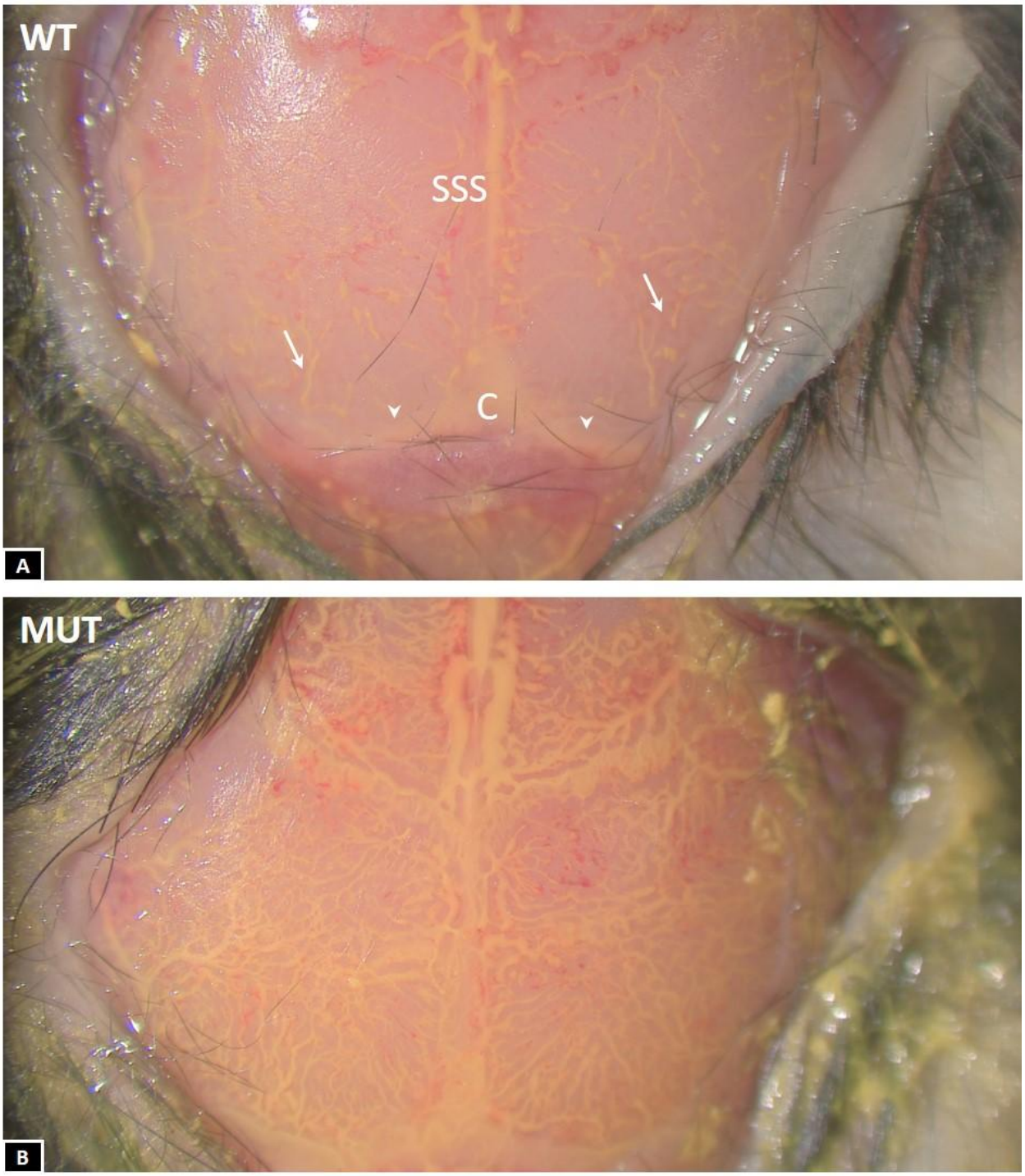

Figure e1. Vascular Microfil Perfusion End-Point. Perfusion with 20% Microfil was continued until the dural sinus and diploic veins were filled completely. **Panel A:** Complete filling of the superior sagittal sinus (SSS), confluens (C), transverse sinuses (arrowhead), and diploic veins (arrows) is used as the end-point for Microfil vascular perfusion in the littermate control (WT). The image shown is slightly underfilled, as seen by small regions of remaining blood in the diploic veins. **Panel B:** The same is performed for the transgenic mouse model (MUT).

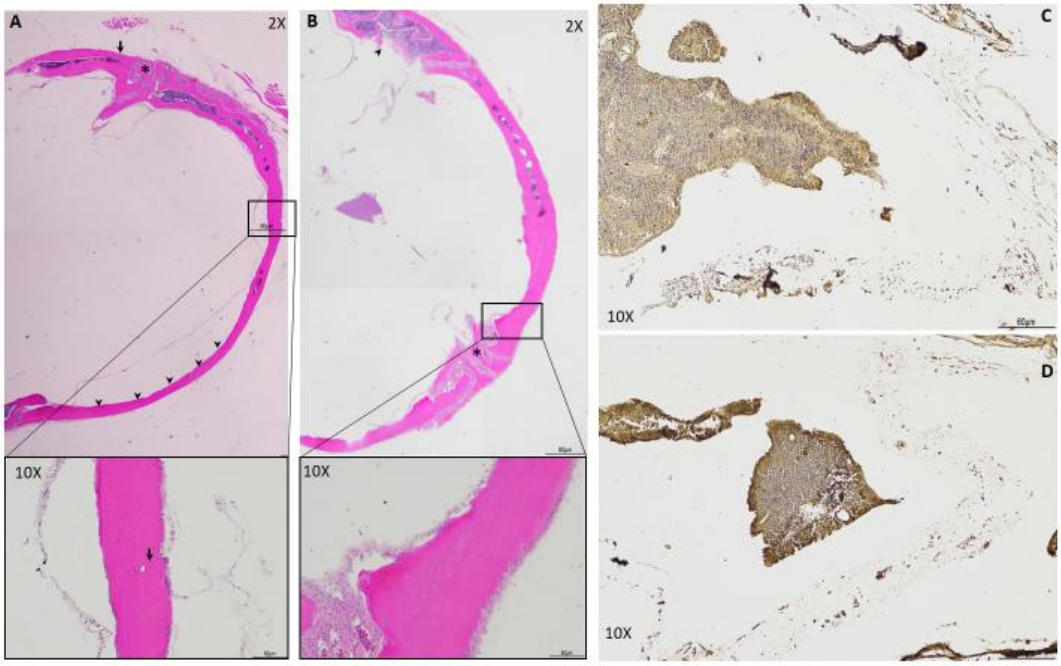

Figure e2. Histology of EPAS1-Gain-of-Function Syndrome mouse model Calvarium. **Panel A:** Representative sections of EPAS1-gain of function mutant mouse model hematoxylin and eosin stained histology of the calvarium at the level of the lambdoidal suture (asterisk) at 2X magnification demonstrates a lack of bone marrow (arrowheads) throughout transitional cartilage. A lack of distinction between periosteum and cartilage is also noted (arrow). 10X magnification of boxed region in panel A demonstrates laminar arrangement of transitional cartilage with poor distinction from and connections to surrounding mesenchyme (arrow). **Panel B:** Littermate control 2X magnification in the same location compared to the mutant. Lambdoidal suture (asterisk). Normal appearing bone marrow pattern (arrowhead). 0X magnification of the boxed region in panel C demonstrates organized bone with distinction from surrounding periosteum. **Panel C:** Immunohistochemistry with the HIF-2α antibody of the bone marrow adjacent to a suture in the control calvarium at 10X magnification. **Panel D:** Immunohistochemistry with the HIF-2α antibody in the same anatomic location and same magnification as the control demonstrates strongly positive staining of the bone marrow compared to the control.

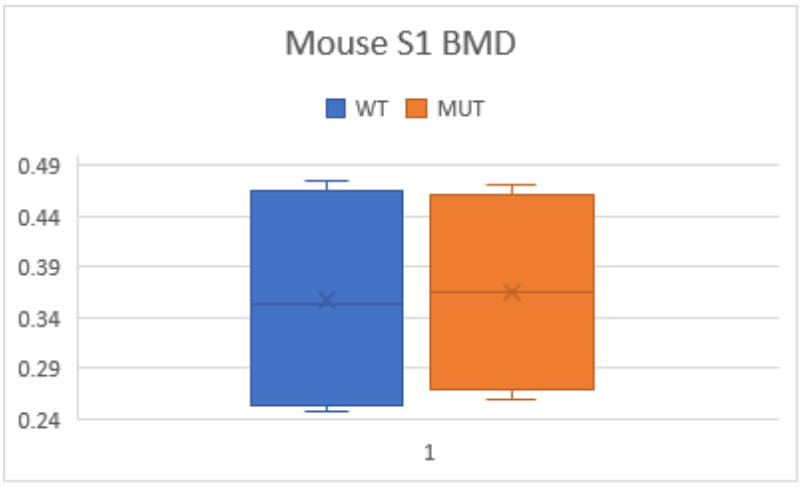

WT	MUT
0.247685	0.259751
0.273409	0.298984
0.47581	0.471823
0.434935	0.432961

Figure e3. Sacral (S1) bone mineral density in EPAS1-Gain-of-Function Mouse Model. WT and MUT mice were evaluated via CT. No significant difference was found between the two groups; $t(3) = 1.15$, $p = 0.17$

Section 3

Patient Posterior Fossa Measurements

Patient #1

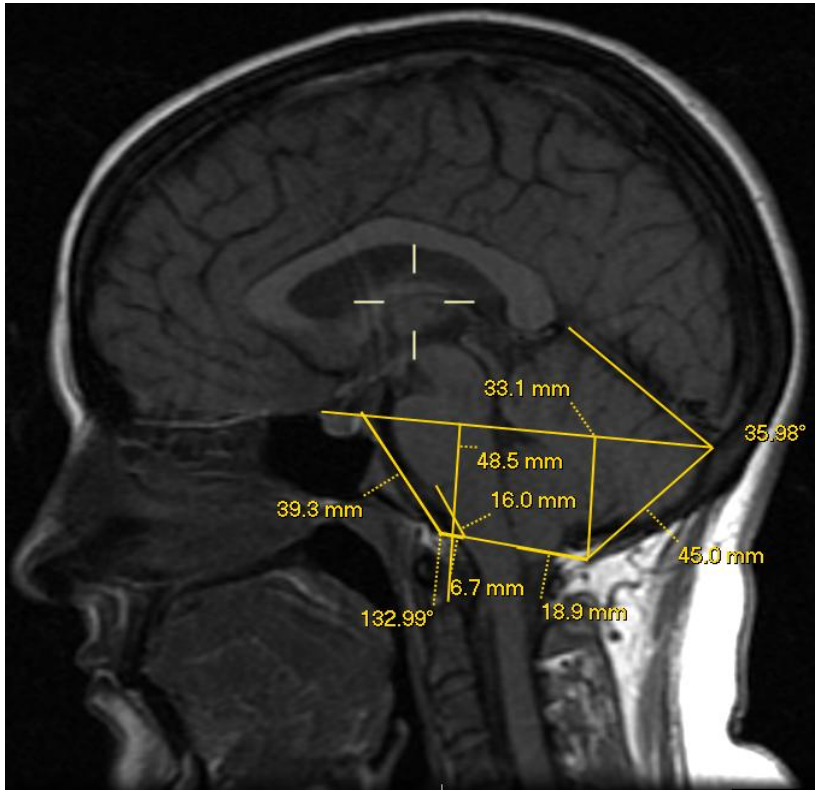
33.1 mm
35.98°
48.5 mm
39.3 mm
16.0 mm
45.0 mm
6.7 mm
132.99°
18.9 mm

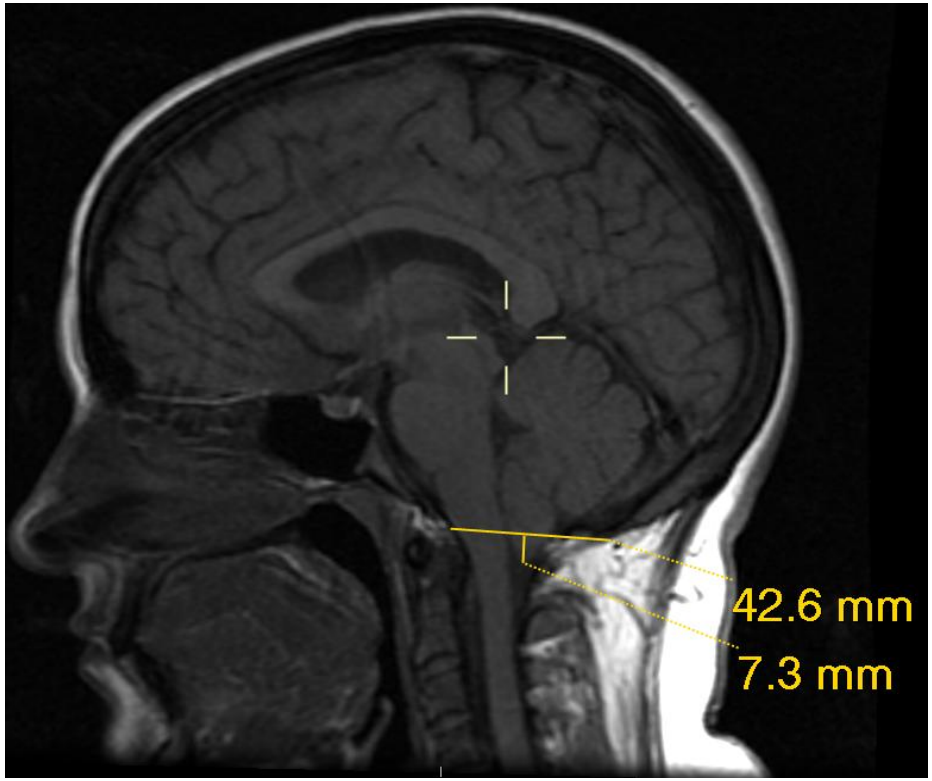
42.6 mm
7.3 mm

Patient #2

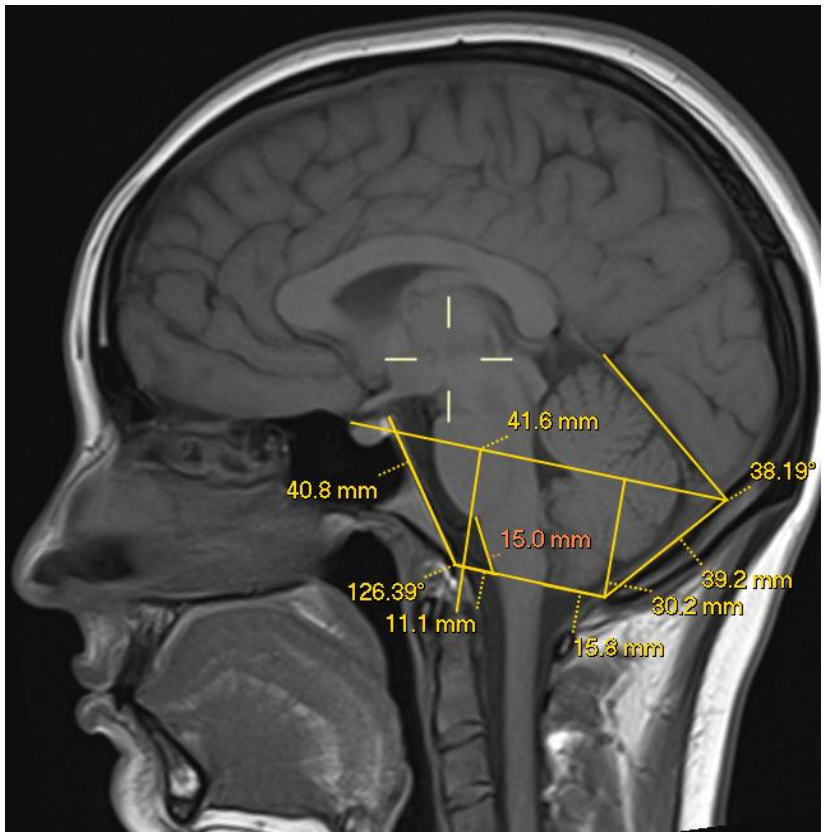
41.6 mm
40.8 mm
38.19°
15.0 mm
126.39°
11.1 mm
39.2 mm
30.2 mm
15.8 mm

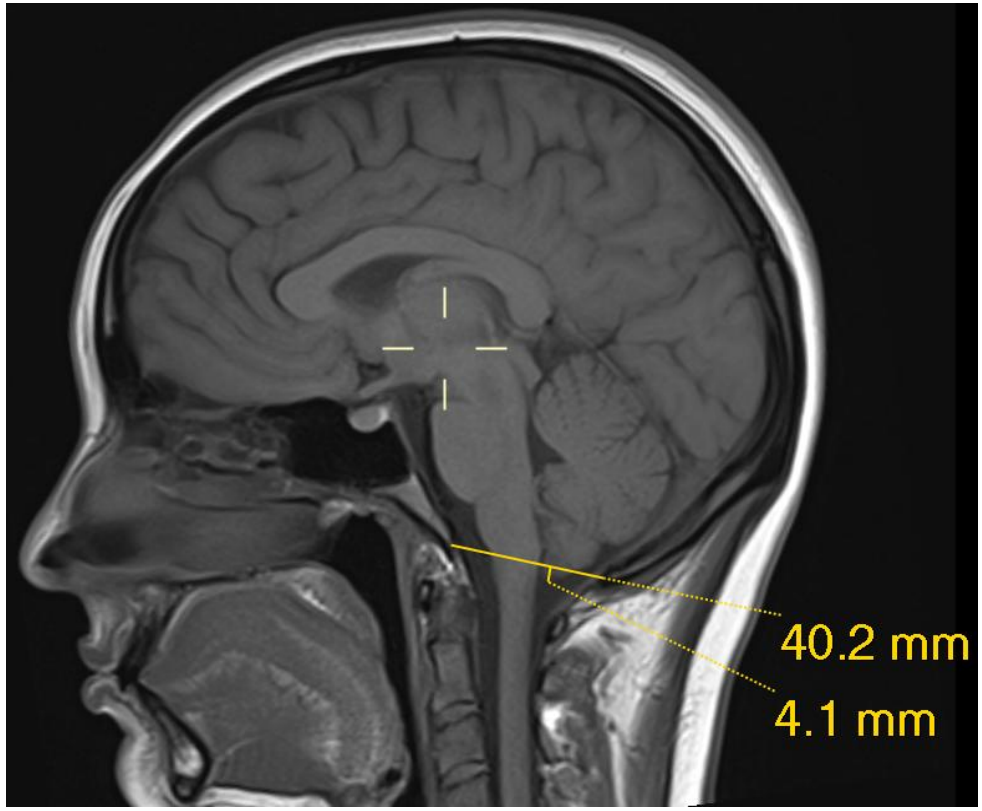
40.2 mm
4.1 mm

Patient #3

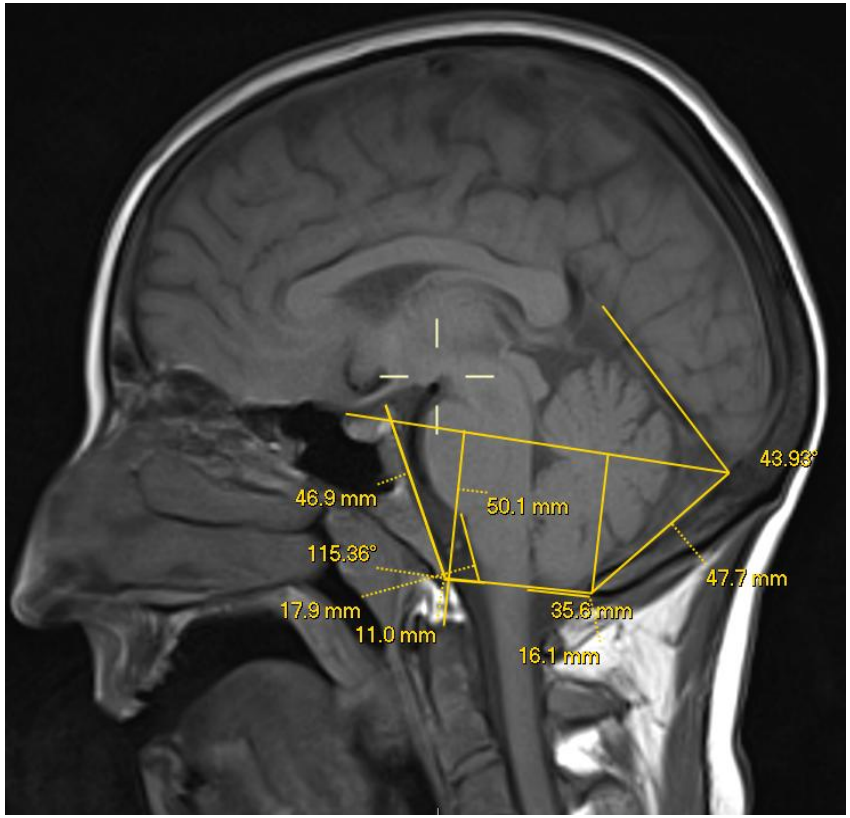
43.93°
46.9 mm
50.1 mm
115.36°
47.7 mm
17.9 mm
11.0 mm
35.6 mm
16.1 mm

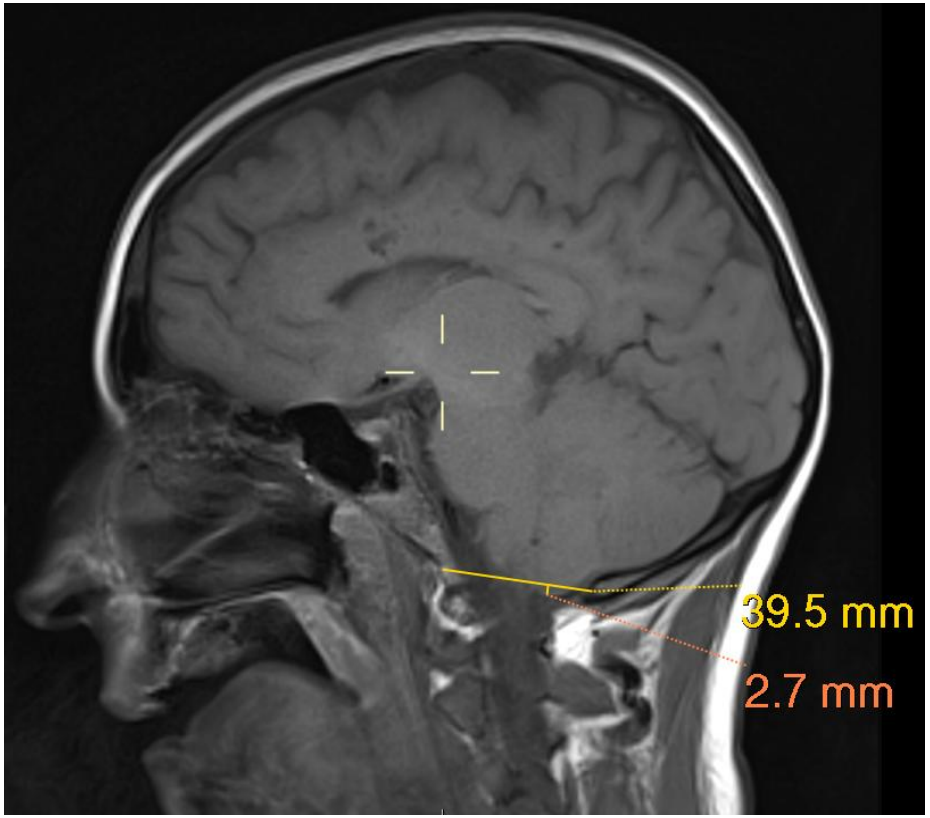
39.5 mm
2.7 mm

Patient #4

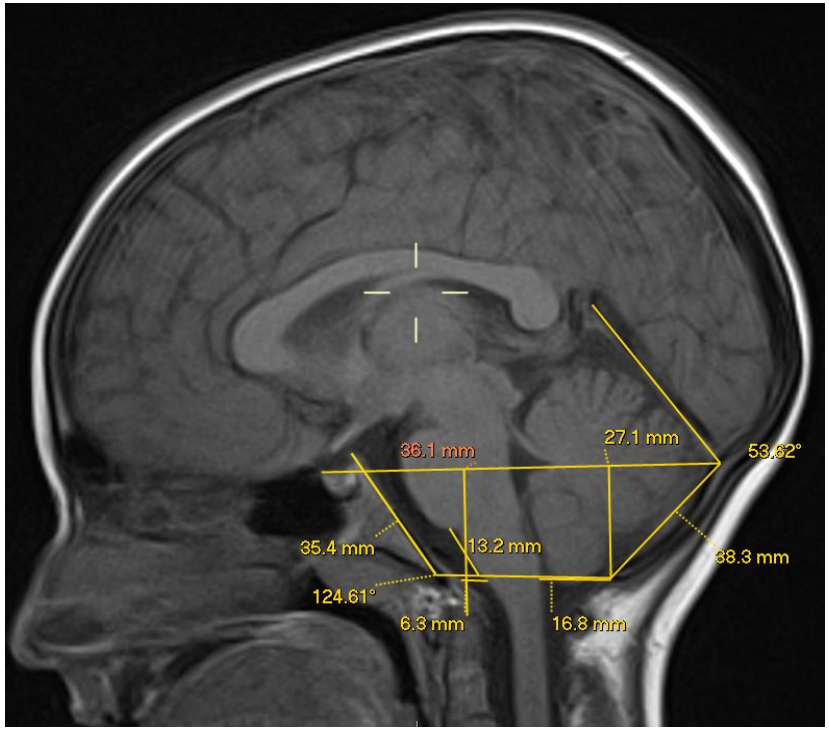
36.1 mm
27.1 mm
53.62°
35.4 mm
13.2 mm
38.3 mm
124.61°
6.3 mm
16.8 mm

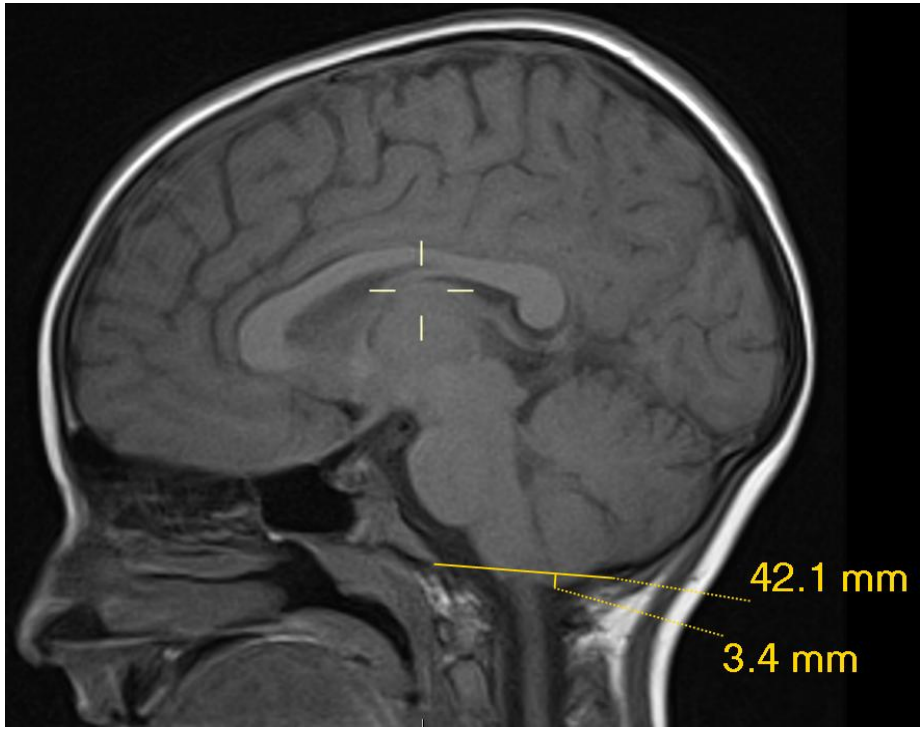
42.1 mm
3.4 mm

Patient #5

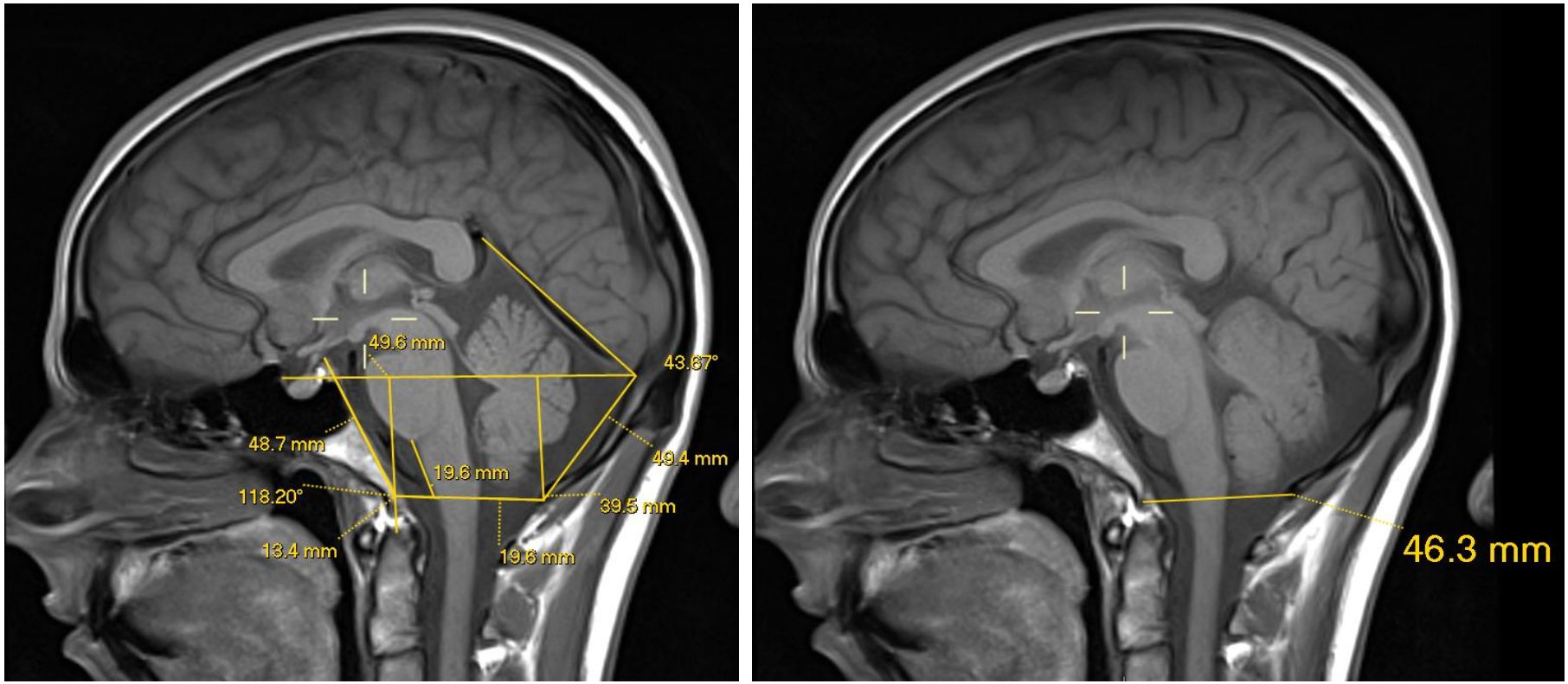

Patient #6

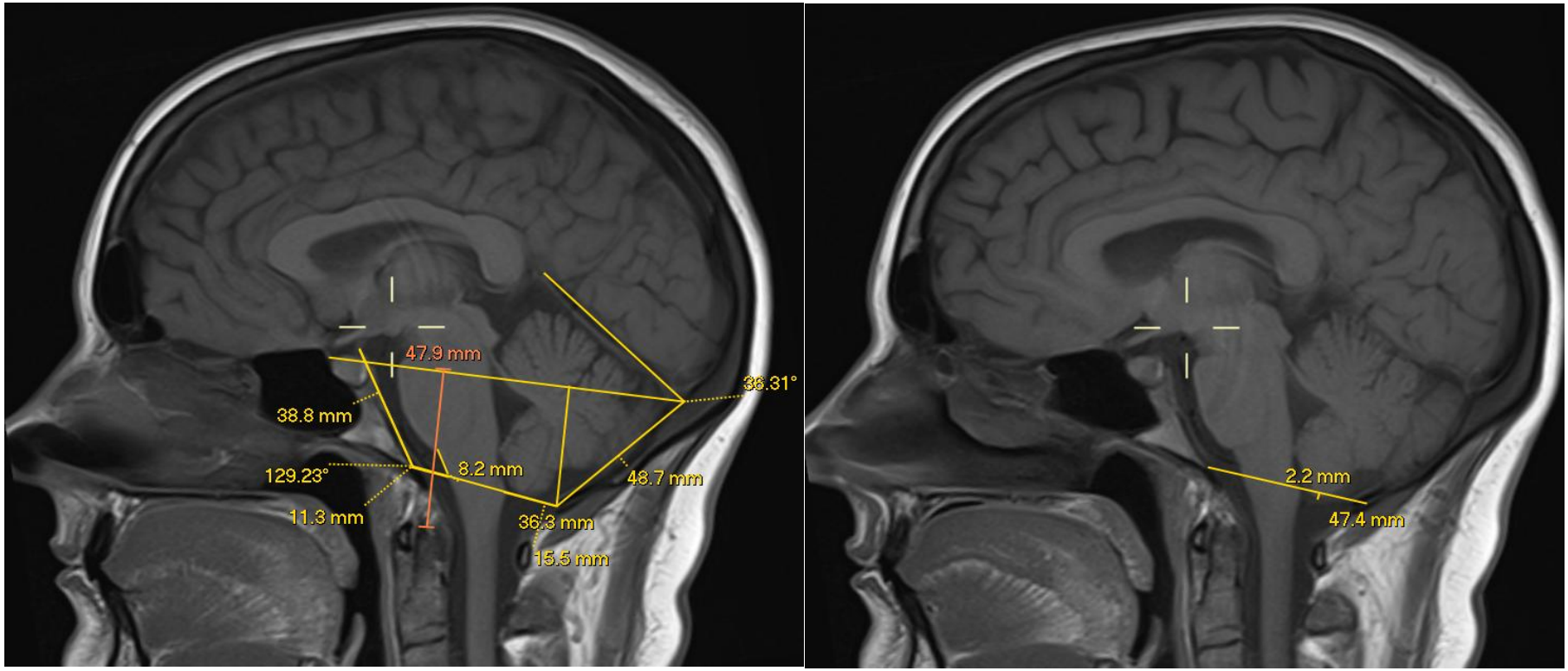
47.9 mm
36.31°
38.8 mm
129.23°
8.2 mm
48.7 mm
11.3 mm
36.3 mm
15.5 mm
2.2 mm
47.4 mm

Patient #7

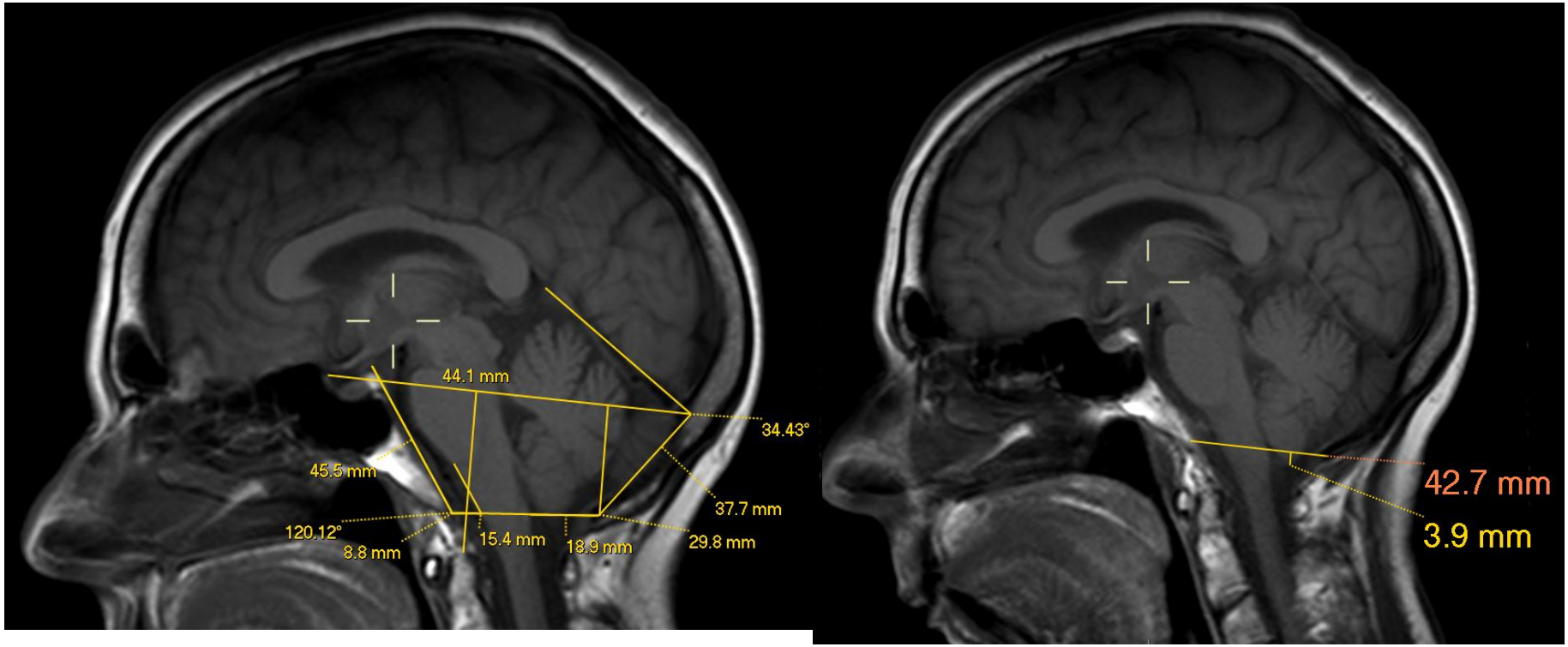
44.1 mm
34.43°
45.5 mm
37.7 mm
120.12°
8.8 mm
15.4 mm
18.9 mm
29.8 mm
42.7 mm
3.9 mm

Patient #8

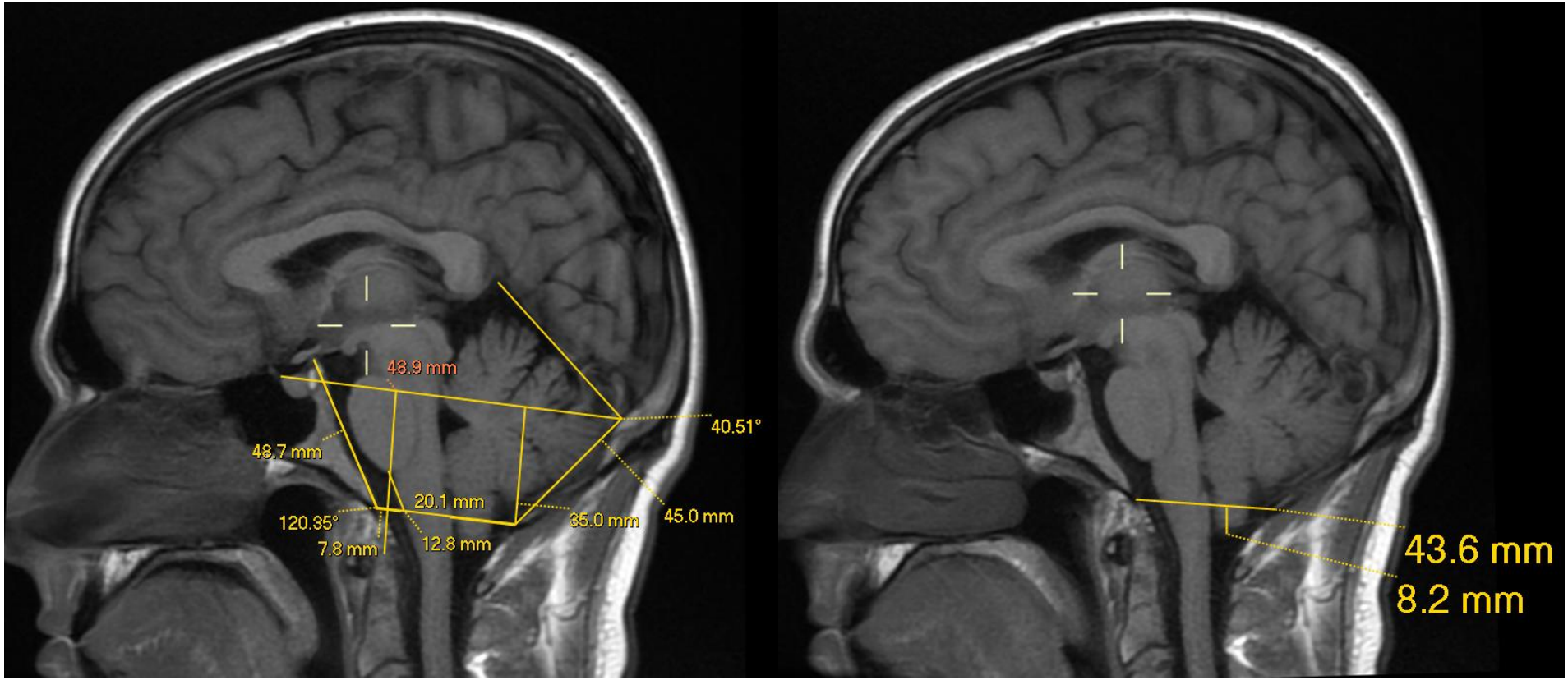
48.9 mm
40.51°
48.7 mm
20.1 mm
120.35°
35.0 mm
45.0 mm
7.8 mm
12.8 mm
43.6 mm
8.2 mm

Section 4

Patient Sacrum Imaging

Chest/Abdomen/Pelvis CT

Patient #1

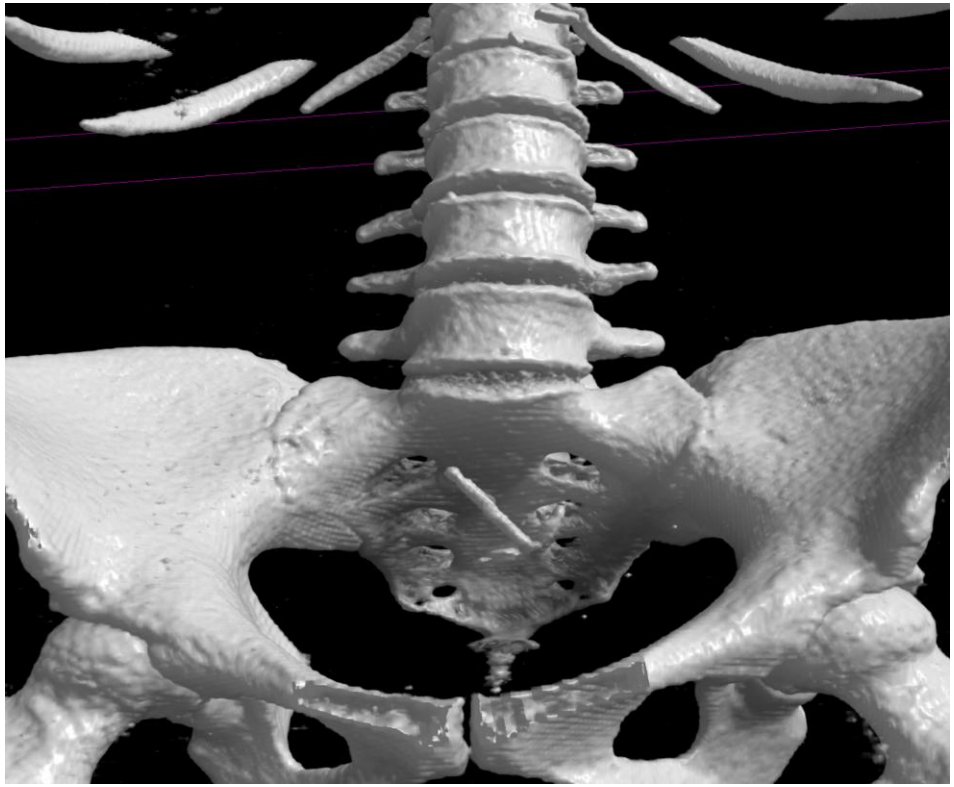

Patient #2

Patient #3

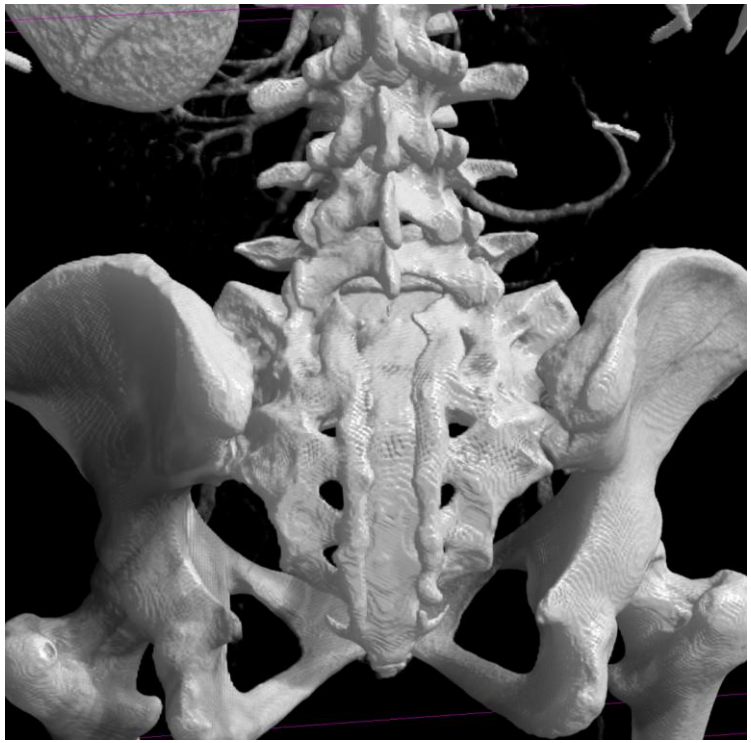

Patient #4

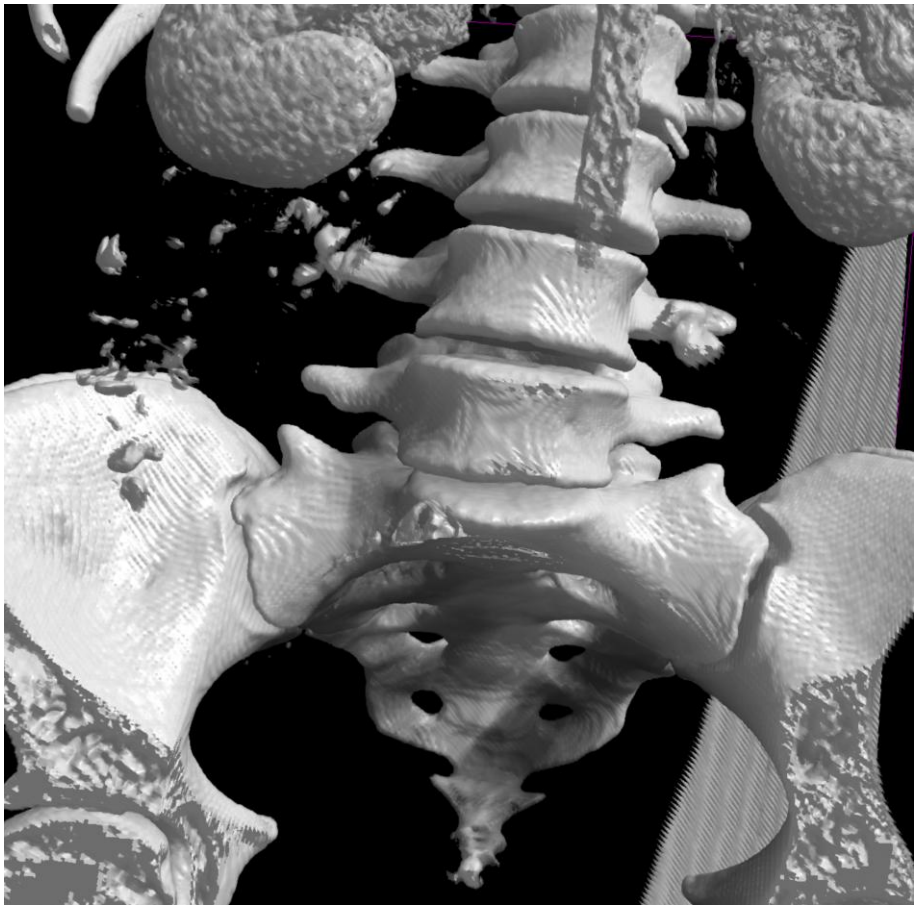

Patient #5

Patient #6

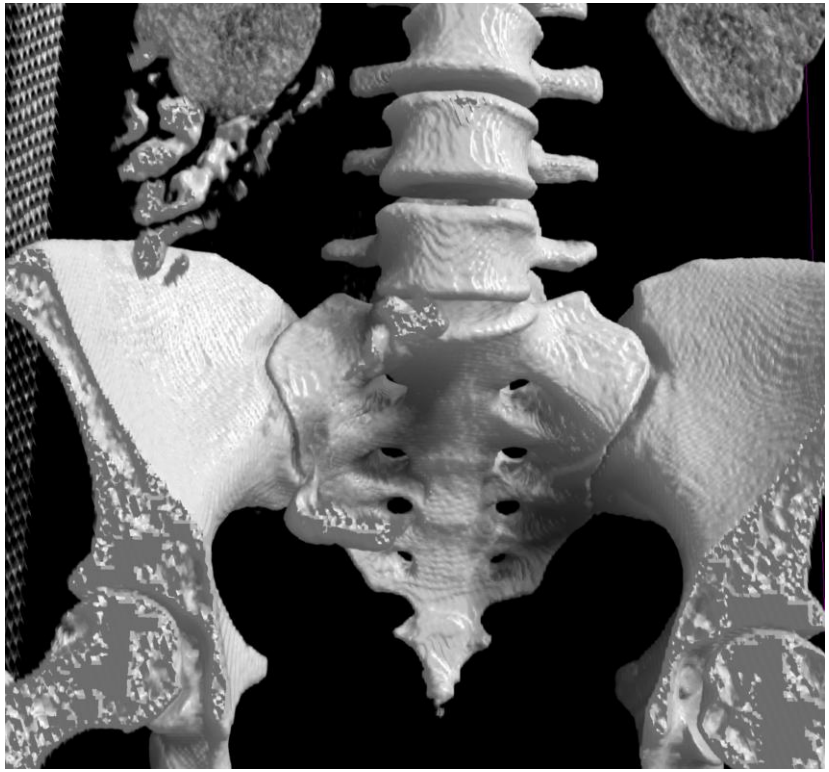

Patient #7

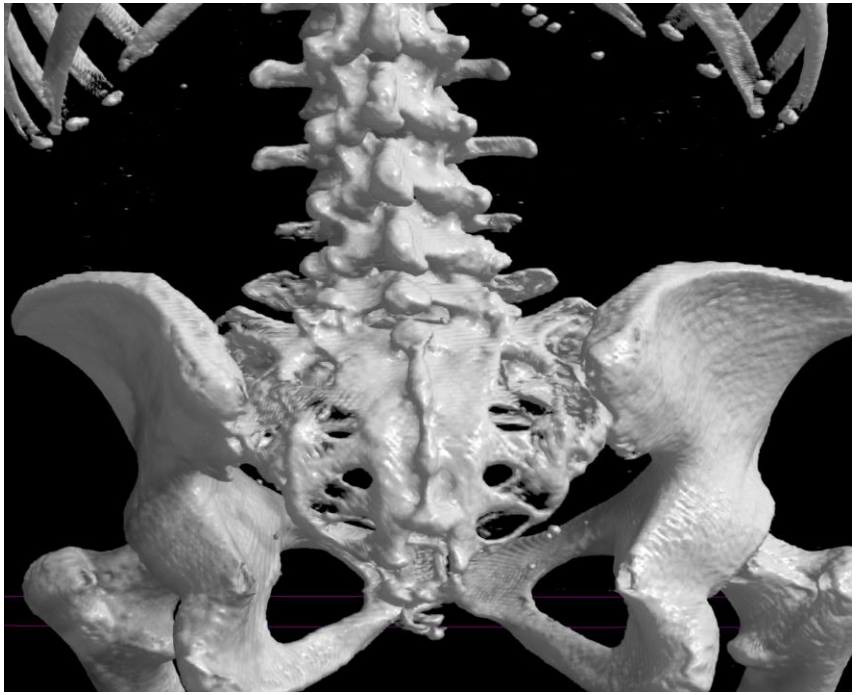

Patient #8

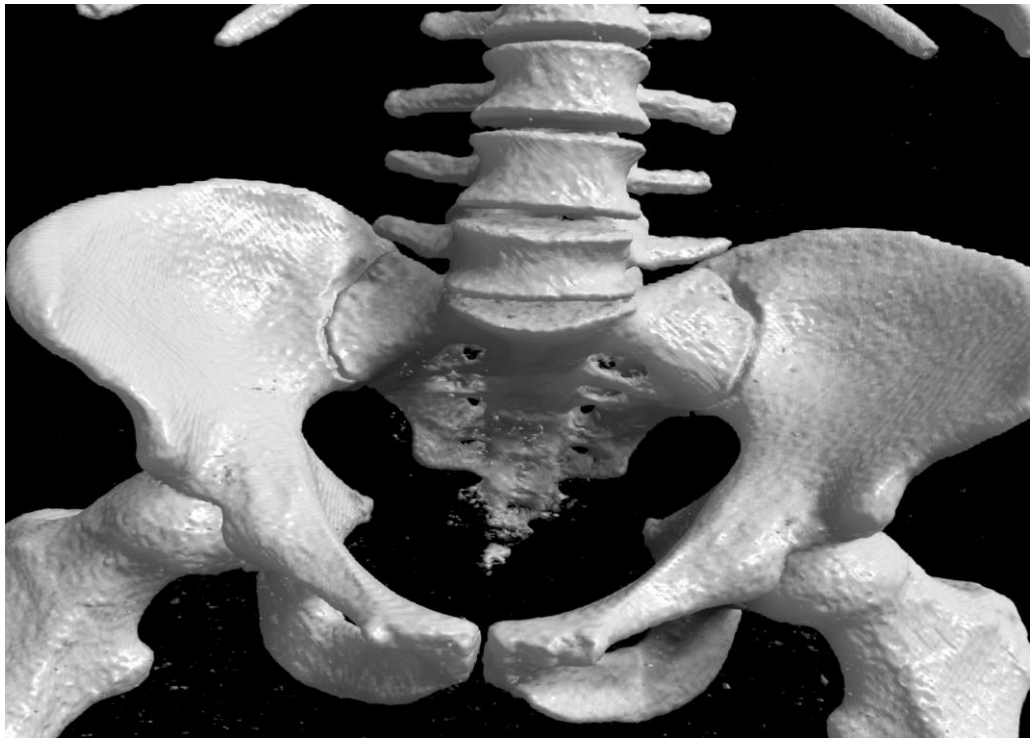

Section 5

Mouse Sacrum Imaging

Micro-CT

Sample #1 (Control)

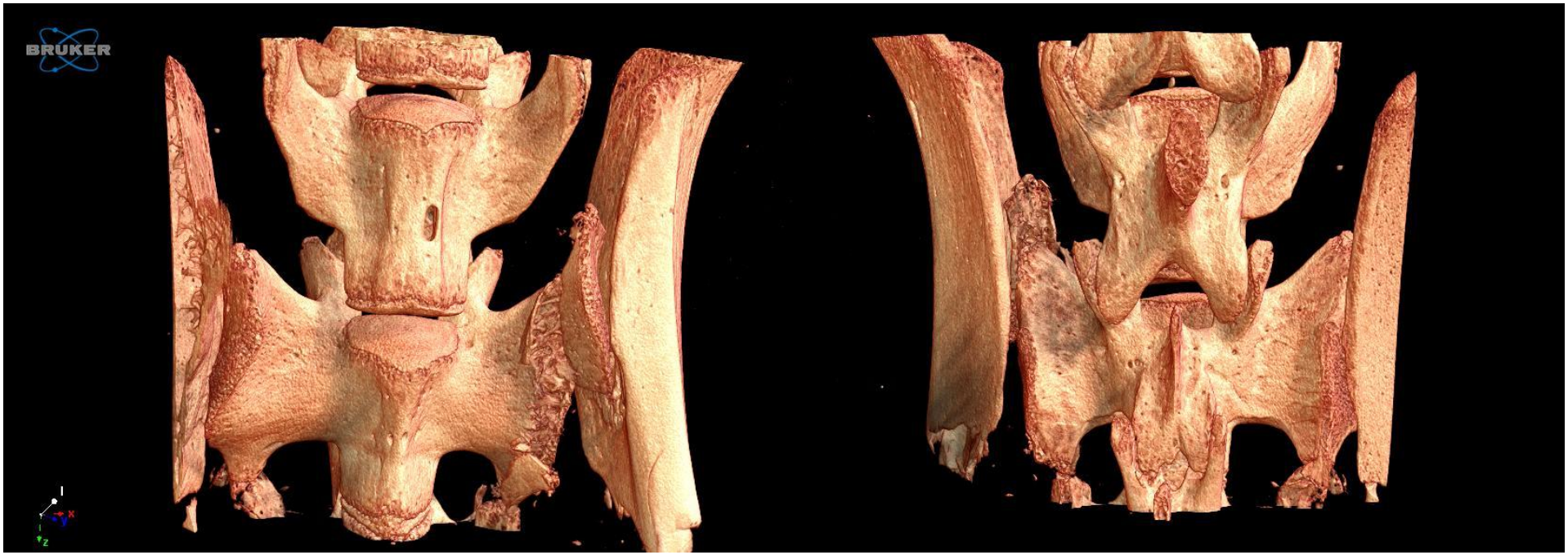

Sample #2(Mutant)

PA view of mutant mouse (Sample #2) sacrum demonstrates linear region of hypodensity in one of the ossification zones of the S1 alae (arrow)

Sample #3 (Control)

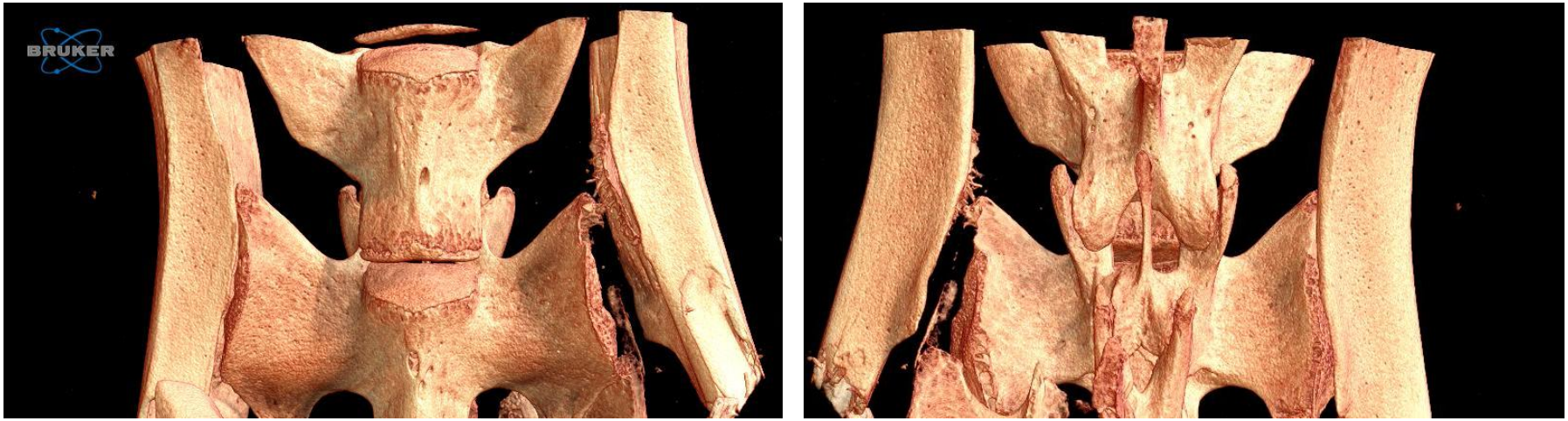

Sample #4 (Mutant)

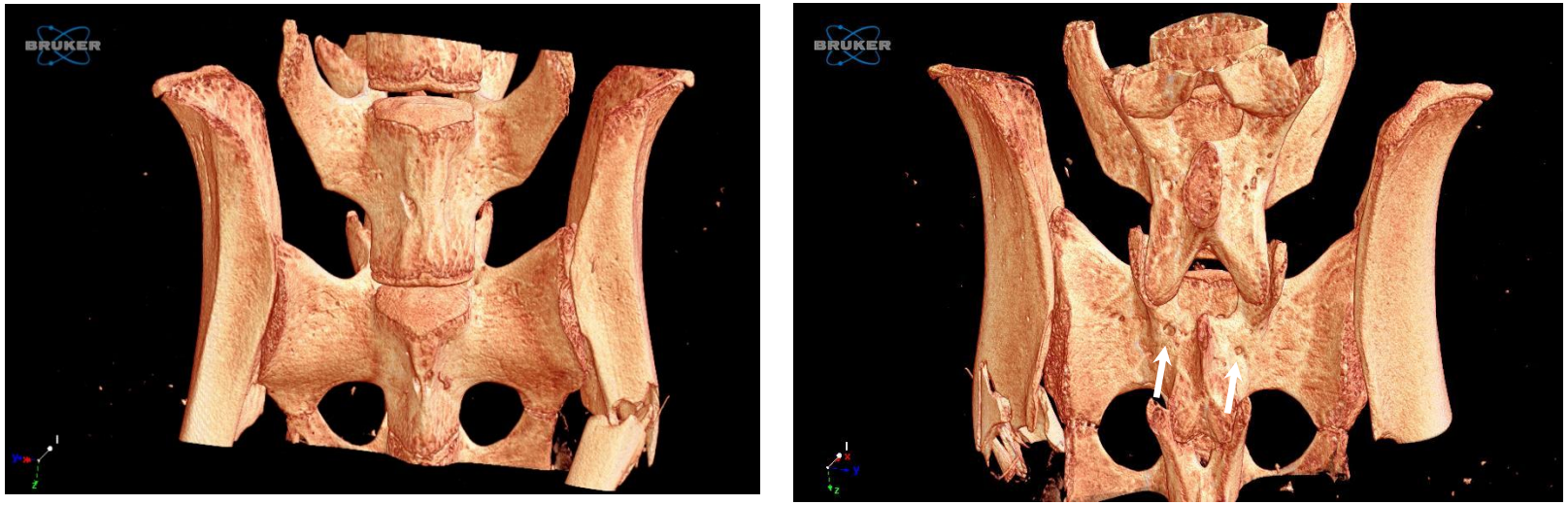

PA view of mutant mouse (Sample #4) sacrum demonstrates dysraphic processes in the lamina of S1 (arrow)

Sample #5 (Control)

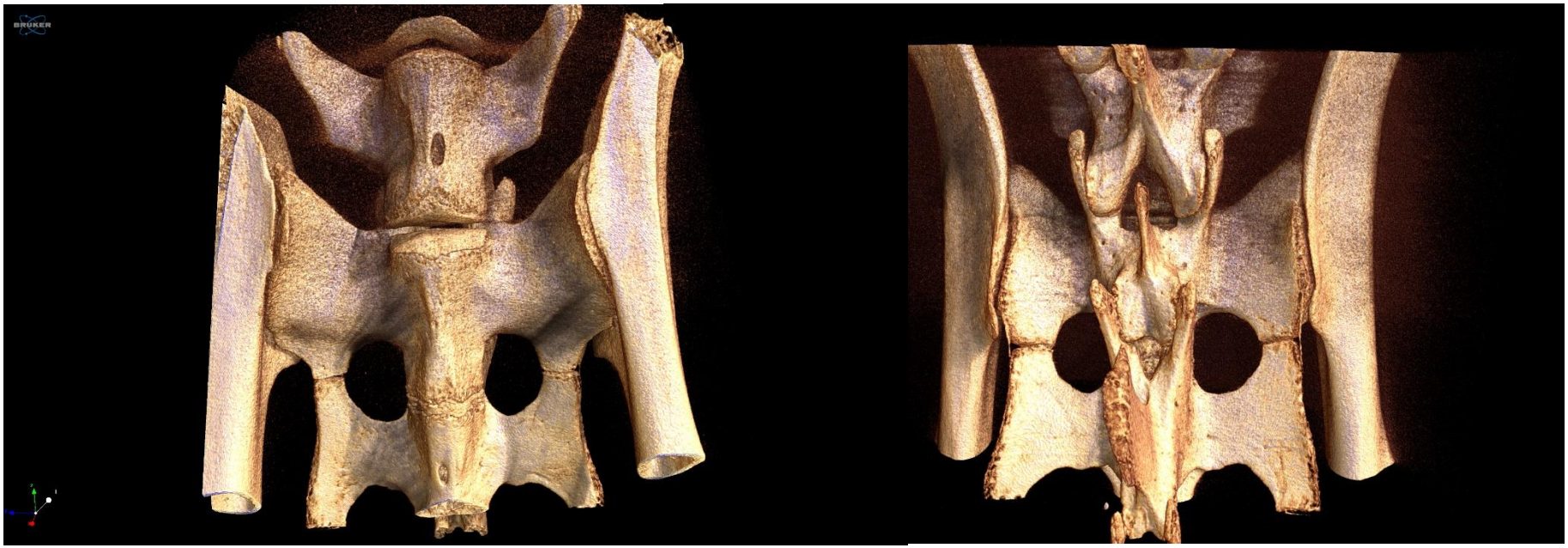

Sample #6 (Mutant)

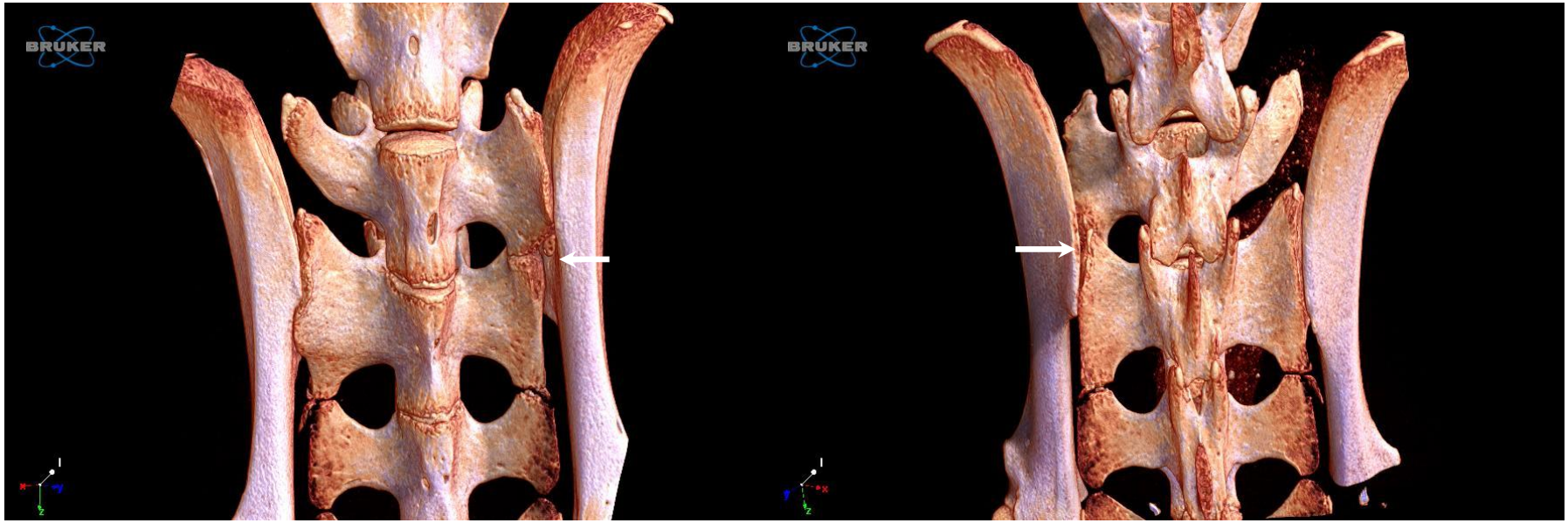

AP and PA view of mutant mouse (Sample #6) sacrum demonstrates abnormal vertebral segmentation of S1(arrow)

Sample #7 (Mutant)

Sample #8 (Control)